

Data-driven Iterative Tuning for Rejecting Spatial Periodic Disturbances Combined with LESO

Xin Huo* Aijing Wu* Ruichao Wang** Kemao Ma*

* *Control and Simulation Center, Harbin Institute of Technology,
Harbin 150080, P.R.China (e-mail: huoxin@hit.edu.cn).*

** *Texas A&M University, College Station, TX 77843, USA.*

Abstract: Iterative learning control (ILC) scheme is known as an effective technique focused on problems which involve repeating tasks, using the error signal from the previous cycle to update the control input. In this paper, a compound control which combines a data-driven iterative turning feedforward controller with a linear extended state observer (LESO) is proposed for spatial periodic disturbances suppression. Due to the problem of feedforward parameter identification in servo system, an algorithm of orthogonal projection is introduced. The error signals caused by the reference trajectory and the disturbances are extracted by projecting the overall error signals onto a subspace spanned by the physical model of the plant as well as the model of the disturbances. Moreover, a data-driven approach is proposed to design the learning gain. Furthermore, a 4th-order LESO is designed to estimate non-periodic disturbances and uncertain dynamics so as to reduce the steady state error. Simulation results validate the proposed method and confirm its effectiveness and superiority.

Keywords: Data-driven, Spatial Periodic Disturbances, Iterative Turning, Orthogonal Projection, Linear Extended State Observer, Compound Control

1. INTRODUCTION

Rotating mechanical systems are widely applied to many practical applications, such as disk actuators, robot manipulators, testing tables and industrial manufacturing. With respect to these kinds of systems, high operation smoothness is a significant index, which is influenced mostly by various disturbances and uncertainties in the systems. Among all these disturbances, periodic disturbances occupy the main position. Some theoretical results can be found in Kalyanam and Tsao (2012); Liu et al. (2018); Guemes et al. (2011).

Iterative learning control (ILC) has found widespread industrial application in control of repetitive processes. In a repetitive process, information from earlier iterations can be used to improve performance in the current iteration. ILC has been implemented in several industrial processes because of its simplicity of design, analysis and implementation. Vast literature associated with ILC exists and it spans both, the theory and the practice, Ahn et al. (2007); Xu and Tan (2003), and references therein. Besides, ILC is suitable for complex system model building and high-precision control. Excluding the effect of model uncertainty, data-driven ILC is popular when an accurate dynamic model is not available. Stearns et al. (2008) iteratively tuned the feedforward controller to compensate the force ripple disturbances of a wafer stage. Tousain et al. (2001) established the closed-loop model of the iterative algorithm based on the pulse transfer matrix of the plant,

* This work was supported by National Nature Science Foundation (NNSF) of China under Grant 61773138.

and used the optimal method of multi-objective functions to design the learning gain, so as to achieve optimal tracking performance under the premise of the stability in iterative domain with a certain robustness. Although many scholars at home and abroad have adopted ILC for disturbance suppression, parameter identification and achieved good results, there still exist the following limitations: the iterative algorithm only performs in time domain, where its coupled parameters affect the identification process. Orthogonal projection is therefore introduced to avoid such problems, and in this way what need to be identified is merely the parameters projected onto the subspace formed by the basis functions, thus greatly compresses the identification matrix, reduces the algorithm complexity.

However, in many practical systems, the periodicity of the system does not exist in time interval, but in space interval. Many uncertainties or external disturbances of a moving system are functions of spatial position or system state rather than time Huo et al. (2016). In addition to spatial periodic disturbances, there also exist other uncertain disturbances and unknown dynamics in rotary machines, whose characteristics are hard to model. Recently, active disturbance rejection control (ADRC) has been well developed and achieved satisfactory performance for uncertain systems, which is symbolized by the use of linear extended state observer (LESO), investigated in Dan and Chen (2009); Han (2009); Huang and Xue (2014). Focused on estimating and compensating the total disturbance or total uncertainty, ADRC concentrates on the effects of external disturbances and unknown dynamics on the output. Besides, some valuable state information

can be obtained with ESO such as the angular velocity, which may save the computation resources.

In this paper, motivated by the suppression of spatial periodic and uncertain disturbances, a compound control method which combines a data-driven iterative tuning feedforward controller with a LESO is proposed. The ILC algorithm uses only partial error information from the previous iteration, which is obtained by projection of the entire error information vector onto a smaller subspace spanned by a set of basis functions. It is motivated by the physical model of repetitive disturbances along with the trajectory to be tracked. Further, a fourth-order LESO is designed to deal with remained uncertain disturbances which still degrade the performance of the ILC scheme. The following theoretical results proposed in this paper are carried on a turntable system, as shown in Fig. 1.



Fig. 1. Turntable system

The rest of the paper is organized as follows. Section 2 analyzes and builds the models of both the plant and the disturbances. The projection algorithm is briefly introduced as well. In Section 3, a data-driven ILC algorithm based on the orthogonal projection as well as its convergence analysis is given. Whereafter, a method of compound control design using LESO is proposed along with its parameters' adjustment. Simulation and comparison results are provided in Section 4 to show the effectiveness of the proposed method. Concluding remarks are given in Section 5.

2. PROBLEM FORMULATION

2.1 Mathematical model

The turntable system considered in this paper is driven by a permanent magnet synchronous motor (PMSM) with vector control, which is realized through angular position closed-loop. The motion model of the PMSM can be described by

$$J \frac{d\omega}{dt} = T_m - D\omega - T_l \quad (1)$$

where ω is angular velocity of the motor, T_m is the electromagnetic torque, T_l is the load torque, J is the inertia and D is the drag coefficient.

The model in (1) can be described by Fig. 2, where i_c is the control current signal, θ is the output angular position, R is the stator resistance, L is inductance, K_s is the equivalent gain of driving circuit, K_e is back electromotive force coefficient and K_m is torque coefficient of PMSM. From Fig. 2, without considering the load torque T_l , the

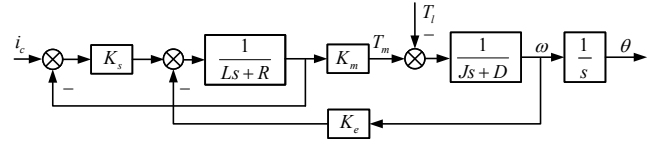


Fig. 2. Block diagram of the PMSM system

transfer function of the plant in Laplace domain can be given as follows,

$$G(s) = \frac{K_m K_s}{LJs^2 + (RJ + K_s J + DL)s + (DR + DK_s + K_m K_e)} \cdot \frac{1}{s} \quad (2)$$

As wind resistance is usually small, the drag coefficient D can be ignored. With $D=0$, (2) is simplified as

$$G(s) = \frac{K}{\tau_m \tau_e s^2 + \tau_m s + 1} \cdot \frac{1}{s} \quad (3)$$

where $\tau_e = \frac{L}{K_s + R}$ and $\tau_m = \frac{J(K_s + R)}{K_m K_e}$ are the electrical time constant and electromechanical time constant, respectively. $K = \frac{K_s}{K_e}$ is the equivalent magnification.

2.2 Disturbance analysis

According to the analysis in Yao et al. (2013); Ou et al. (2018); Huo et al. (2020), we know that the frequencies of disturbances of the turntable system are mainly caused by torque disturbances due to the unbalancing loading and the torque ripples of the motor. The motor torque ripples are divided into electromagnetic torque ripple and cogging torque ripple, which are determined by the number of pole-pairs and tooth-slots.

The accurate model of disturbances is intractable due to the mechanism of the uneven distribution of the body mass and the ripples of the PMSM, it can be modeled as periodic functions in form of the angular position, that is

$$f_{rip} = \sum_{i=1}^m A_i \sin(\hat{\omega}_i \theta + \phi_i) \quad i = 1, \dots, m \quad (4)$$

where θ is the angular position of the motor, A_i , ϕ_i and $\hat{\omega}_i$ are the amplitude, phase angle and spatial frequency of the i th major disturbance harmonics, respectively.

2.3 Orthogonal Projection

Define $f_1(t), f_2(t), \dots, f_n(t)$ as the orthogonal basis functions of the subspace H , the projection of signal $u(t)$ onto the subspace H can be given as

$$u(t)|_H = \xi_1 f_1(t) + \xi_2 f_2(t) + \dots + \xi_n f_n(t) = \mathbf{f}(t)\boldsymbol{\xi} \quad (5)$$

where $\mathbf{f}(t) \triangleq [f_1(t), f_2(t), \dots, f_n(t)]$, $\boldsymbol{\xi} \triangleq [\xi_1, \xi_2, \dots, \xi_n]^T$. $\boldsymbol{\xi}$ denotes the vector representation of $u(t)$ in the subspace H , which can be calculated by

$$\boldsymbol{\xi} = \langle \mathbf{f}(t), u(t) \rangle \quad (6)$$

where \langle, \rangle denotes the inner product operation, i.e., $\langle \mathbf{x}(t), \mathbf{y}(t) \rangle = \int \mathbf{x}(t)\mathbf{y}(t) dt$.

The measured data are available only with the sampling period T_s and the input is injected to the plant through a zero-order hold(ZOH). Therefore, the orthogonal projection matrix is obtained as

$$\mathbf{F} \triangleq \begin{bmatrix} f_1(0) & f_2(0) & \dots & f_n(0) \\ f_1(T_s) & f_2(T_s) & \dots & f_n(T_s) \\ \vdots & \vdots & \dots & \vdots \\ f_1(NT_s) & f_2(NT_s) & \dots & f_n(NT_s) \end{bmatrix} \quad (7)$$

For a vector $\mathbf{x}^j \in R^N$, the superscript j denotes the iteration index of the experiment. It is defined as $\mathbf{x}^j = [x^j(0)x^j(1) \cdots x^j(N-1)]$, where $x^j(k)$ is a measurement at time instant k for $k = 0, 1, \dots, N-1$ with N being the number of samples. The symbols q and z denote the forward shift operator with respect to time and iteration, respectively. Namely, $qx(k) = x(k+1)$ and $zx^j = x^{j+1}$.

3. MAIN RESULTS

In this section, we propose a compound control scheme to suppress various kinds of disturbances, especially the disturbances which are angular position dependent. Due to the effectiveness of ILC in suppressing spatial periodic disturbances, we project the error data onto a subspace to capture the effective error information caused by the reference and disturbances. A data-based gradient approach is proposed to design the learning gain. Moreover, the LESO is used to estimate and compensate for other remained disturbances as well as uncertain dynamics.

3.1 Data-driven ILC based on orthogonal projection

The identification is performed by using a feedforward controller until the tracking error cannot be reduced. The data-driven ILC structure is shown in Fig. 3, where $K(s)$ is the feedback controller, r is the reference input and u_{ff}^j is the feedforward control signal. The position output $y^j(\theta)$ is affected by periodic disturbances f_{rip}^j as well as uncertain ones f_d^j .

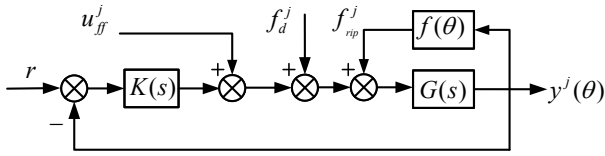


Fig. 3. Configuration of data-driven ILC system

From Fig. 3, the tracking error in Laplace domain can be given as

$$e^j(s) = \frac{r - (f_{rip}^j + u_{ff}^j)G}{1 + KG} - \frac{Gf_d^j}{1 + KG} \quad (8)$$

$$= e_0^j(s) + e_d^j(s)$$

with

$$\begin{cases} e_0^j(s) = S(s)r - G(s)S(s)(f_{rip}^j + u_{ff}^j) \\ e_d^j(s) = -G(s)S(s)f_d^j \end{cases} \quad (9)$$

where $S(s) = \frac{1}{1+KG}$ is the sensitivity function of the feedback loop. It follows that if $u_{ff}^j = G^{-1}r - f_{rip}^j$, $e_0^j = 0$.

For the convenience of identification, (3) and (4) can be simplified as

$$G(s) = \frac{1}{a_1s^3 + a_2s^2 + a_3s} \quad (10)$$

$$f_{rip} = \sum_{i=1}^m [\alpha_i \sin(\hat{\omega}_i\theta) + \beta_i \cos(\hat{\omega}_i\theta)] \quad (11)$$

where a_1, a_2 and a_3 are the corresponding coefficients after simplification. Thus, the desired feedforward term in time domain can be expressed as

$$u_{ff}^*(t) = a_1 \frac{d^3r}{dt^3} + a_2 \frac{d^2r}{dt^2} + a_3 \frac{dr}{dt} - \sum_{i=1}^m [\alpha_i \sin(\hat{\omega}_i r) + \beta_i \cos(\hat{\omega}_i r)] \quad (12)$$

$$= \varphi(t)\sigma^*$$

where $u_{ff}^*(t)$ is the desired feedforward, σ^* are the true parameters in the model.

$$\begin{cases} \varphi(t) = \left[\frac{d^3r}{dt^3}, \frac{d^2r}{dt^2}, \frac{dr}{dt}, -\sin(\hat{\omega}_1 r), \dots, -\cos(\hat{\omega}_m r) \right] \\ \sigma^* = [\alpha_1, \alpha_2, \alpha_3, \alpha_1, \dots, \alpha_m, \beta_1, \dots, \beta_m]^T \end{cases} \quad (13)$$

The above equations imply that we could seek $u_{ff}^*(t)$ in the finite dimensional subspace H .

$$H = \text{span} \left\{ \frac{d^3r}{dt^3}, \frac{d^2r}{dt^2}, \frac{dr}{dt}, -\sin(\hat{\omega}_1 r), \dots, -\cos(\hat{\omega}_m r) \right\} \quad (14)$$

Since the true parameters σ^* are unknown, the feedforward term $u_{ff}^j(t)$ is parameterized in the following form with estimated $\hat{\sigma}^j$.

$$u_{ff}^j(t) = \varphi(t)\hat{\sigma}^j \quad (15)$$

The essence of orthogonal projection is to pre-compress the state signal. By projection transformation, the time-domain signal can be transformed into the vector space composed of the basis functions and the iterative identification of parameters could then be implemented.

Substituting (12) into (8), it follows that $e_0^* = Sr - GS\varphi\sigma^*$. Therefore, we have

$$Sr = GS\varphi\sigma^* \quad (16)$$

Since the model of the plant G and the sensitivity function S are both unknown, it is impossible to construct GS directly. Let G_B denote the Toeplitz matrix corresponding to GS with the following form.

$$G_B = \begin{bmatrix} g_0 & 0 & \cdots & 0 \\ g_1 & g_0 & \cdots & 0 \\ \vdots & \vdots & \vdots & \vdots \\ g_{N-1} & g_{N-2} & \cdots & g_0 \end{bmatrix} \quad (17)$$

The impulse response only depends on the transfer function of the system. Though it may be affected by other disturbances, this effect can be greatly reduced by matrix operation, since the structure of the fixed system is invariable Mishra and Tomizuka (2009). It could be obtained by injecting an impulse feedforward signal and a zero reference to the system. Substituting (16) into (8), it follows that

$$e_0^j = \varphi(\sigma^* - \hat{\sigma}^j) \quad (18)$$

Define Φ as the digital form of $\varphi(t)$. Φ could be orthogonal decomposed through QR decomposition.

$$\Phi = QR \quad (19)$$

where $R \in R^{n \times n}$ is a nonsingular upper triangular matrix and $Q \in R^{N \times n}$ satisfies $Q^T Q = I^{n \times n}$. Each column of Q constitutes the orthogonal basis of the subspace H . Then δ^j , the coordinate parameters of tracking error e^j in subspace H , could be denoted as

$$\delta^j = Q^T e^j \quad (20)$$

Combining (20) and (18), we have

$$\delta^j = M(\sigma^* - \hat{\sigma}^j) \quad (21)$$

where

$$M = Q^T G_B \Phi \quad (22)$$

Therefore, we can get the data-based estimation of M . The δ^j contains partial, but the most pertinent information in the error signal. Hence, it is the effective information we would utilize for identification.

Inspired by norm-optimal ILC, in this paper, a gradient approach in the subspace H is proposed to design the learning gain. The cost function is given as follows,

$$\mathbf{J}(\hat{\sigma}^j) = (\delta^j)^T \delta^j \quad (23)$$

For the optimization problem in (23), minimizing $\mathbf{J}(\hat{\sigma}^j)$ by taking the partial derivative with respect to $\hat{\sigma}^j$ and setting it to zero leads to

$$\left. \frac{\partial \mathbf{J}}{\partial \sigma} \right|_{\sigma=\hat{\sigma}^j} = 2 \frac{\partial (\delta^j)^T}{\partial \hat{\sigma}^j} \delta^j = -2M^T \delta^j \quad (24)$$

$$\mathbf{H} \Big|_{\sigma=\hat{\sigma}^j} = 2 \frac{\partial (\delta^j)^T}{\partial \hat{\sigma}^j} \left(\frac{\partial (\delta^j)^T}{\partial \hat{\sigma}^j} \right)^T = 2M^T M \quad (25)$$

Then according to the Gauss-Newton gradient iterative algorithm, we have

$$\begin{aligned} \hat{\sigma}^{j+1} &= \hat{\sigma}^j - \lambda \mathbf{H}^{-1} \left. \frac{\partial \mathbf{J}}{\partial \sigma} \right|_{\sigma=\hat{\sigma}^j} \\ &= \hat{\sigma}^j + \lambda M^{-1} \delta^j \end{aligned} \quad (26)$$

where $\lambda \in (0, 2)$ is the learning step.

Hence, the iterative learning identification algorithm can be obtained as follows,

$$\hat{\sigma}^{j+1} = \hat{\sigma}^j + L \delta^j \quad (27)$$

where $L = \lambda M^{-1}$ is the learning gain.

3.2 Convergence analysis

Substituting (21) into (27), we have

$$\hat{\sigma}^{j+1} = (I - LM) \hat{\sigma}^j + LM \sigma^* \quad (28)$$

Since $\lambda \in (0, 2)$, obviously, we have

$$\rho(I - LM) < 1 \quad (29)$$

where $\rho(A)$ denotes the maximum singular value of A . (29) indicates that the convergence is monotonous. It guarantees monotonic transient convergence as well as bounds the steady state error.

Let z denote the forward shift operator with respect to the iteration index j . From (28), we have

$$\hat{\sigma}^j = [(z - 1)I + LM]^{-1} LM \sigma^* \quad (30)$$

Then the z -domain relationship can be given as follows,

$$\hat{\sigma}(z) = T_{\hat{\sigma}\sigma^*}(z) \frac{z}{z-1} \lambda \sigma^* \quad (31)$$

where $T_{\hat{\sigma}\sigma^*}(z) = [(z - 1)I + LM]^{-1}$. Based on the final value theorem of z -transform, we can get

$$\begin{aligned} E[\sigma^\infty] &= E \left[\lim_{z \rightarrow 1} (z - 1) \lambda \hat{\sigma}(z) \right] \\ &= T_{\hat{\sigma}\sigma^*}(1) \lambda \sigma^* \\ &= \sigma^* \end{aligned} \quad (32)$$

In summary, for the system described above, the proposed iterative learning algorithm is monotonically convergent. Further more, $E[\sigma^j] \rightarrow \sigma^*$, when $j \rightarrow \infty$.

3.3 Compound control design

The data-driven ILC based on orthogonal projection is utilized to suppress the periodic disturbances while other uncertain disturbances still deteriorate the tracking performance. One promising way is ESO. Put forward by Han (2009), ADRC was designed to estimate the total uncertainties online by using ESO. By adding the state feedback and command feedforward to ESO, the control system can obtain steady and dynamic states of high quality. Although the original formulation of ESO has a nonlinear gain structure, LESO has attracted much attention as it is easier to design and simple to implement. So here, a LESO is added into the loop. Configuration of overall system with compound control is shown in Fig. 4.

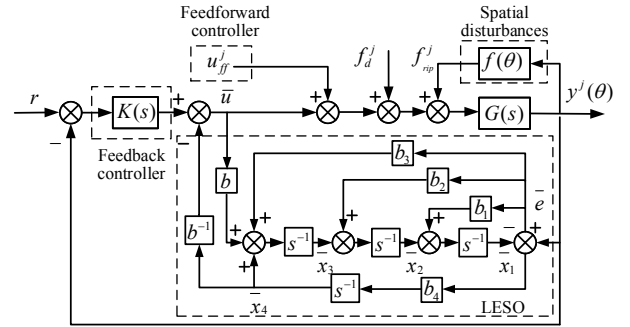


Fig. 4. Configuration of system with compound control

For the 3rd-order plant obtained in (3), a 4th-order LESO is shown

$$\begin{cases} \dot{\bar{x}}_1 = \bar{x}_2 + b_1(y - \bar{x}_1) \\ \dot{\bar{x}}_2 = \bar{x}_3 + b_2(y - \bar{x}_1) \\ \dot{\bar{x}}_3 = \bar{x}_4 + b_3(y - \bar{x}_1) + b\bar{u} \\ \dot{\bar{x}}_4 = b_4(y - \bar{x}_1) \end{cases} \quad (33)$$

where $\bar{x}_1, \bar{x}_2, \bar{x}_3, \bar{x}_4$ are the observer states, \bar{u} is the input of LESO and b is the gain of \bar{u} . Specifically, \bar{x}_4 is the extended state of the output port equivalent disturbance since \bar{x}_1 is the position estimation without disturbance and \bar{x}_2 is the estimate of the angular velocity.

$$b_1 = 4\omega_{eso} \quad b_2 = 6\omega_{eso}^2 \quad b_3 = 4\omega_{eso}^3 \quad b_4 = \omega_{eso}^4 \quad (34)$$

where ω_{eso} denotes the observer bandwidth. In general, the larger the observer bandwidth is, the more effective the observer is. The modified control input is given by

$$\bar{u} = u_0 - \bar{x}_4/b \quad (35)$$

Finally, the discretized LESO is given by

$$\begin{cases} \bar{e}(k) = y(k) - \bar{x}_1(k) \\ \bar{x}_1(k+1) = \bar{x}_1(k) + T_s(\bar{x}_2(k) + b_1\bar{e}(k)) \\ \bar{x}_2(k+1) = \bar{x}_2(k) + T_s(\bar{x}_3(k) + b_2\bar{e}(k)) \\ \bar{x}_3(k+1) = \bar{x}_3(k) + T_s(\bar{x}_4(k) + b_3\bar{e}(k) + b\bar{u}(k)) \\ \bar{x}_4(k+1) = \bar{x}_4(k) + T_s b_4 \bar{e}(k) \\ \bar{u}(k) = u_0(k) - \bar{x}_4(k)/b \end{cases} \quad (36)$$

4. NUMERICAL EXAMPLES

In this section, numerical simulations are presented to illustrate the proposed scheme for the disturbances rejection and evaluate its correctness.

4.1 Simulation set-up

In the illustrated example, the sampling period is $T_s = 500\mu s$, the model of the plant in simulations is

$$G(s) = \frac{92224}{s^2 + 514.5s + 781.1} \cdot \frac{1}{s} \quad (37)$$

Here, a step disturbance and three periodic disturbances are introduced, in which the frequencies of periodic disturbances in spatial domain are

$$\hat{\omega}_1 = \frac{1}{360}/\text{deg}, \quad \hat{\omega}_2 = \frac{1}{24}/\text{deg}, \quad \hat{\omega}_3 = \frac{1}{10}/\text{deg} \quad (38)$$

The selection of stabilizing controller $K(s)$ can be synthesized by the classic loop shaping method as follows,

$$K(s) = 16.2297 \cdot \frac{0.2756s + 1}{0.0919s + 1} \cdot \left(\frac{0.0083s + 1}{0.0049s + 1} \right)^5 \quad (39)$$

For the time-varying command velocity with three stages including acceleration, constant angular velocity and deceleration of the turntable system, a recorded control signal, which indirectly reflects the disturbances, is depicted in Fig. 5 in time domain as well as in spatial domain, respectively. Obviously, the disturbances are periodic in the angular position rather than time.

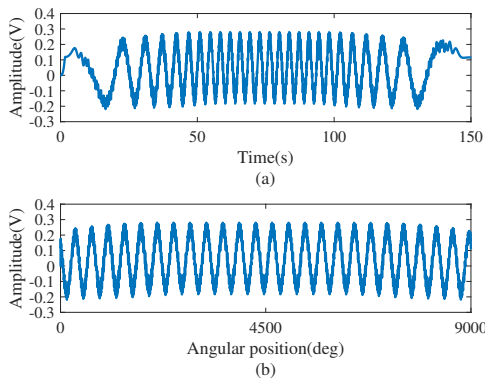


Fig. 5. Control signal in time and spatial domain. (a)Time domain (b)Spatial domain

The learning step λ is selected as 0.7, the plots of estimates versus iterations are shown in Fig. 6. It can be observed that almost all estimates converge to steady constant values after several iterations. Table 1 shows specific information of the true parameters and estimates.

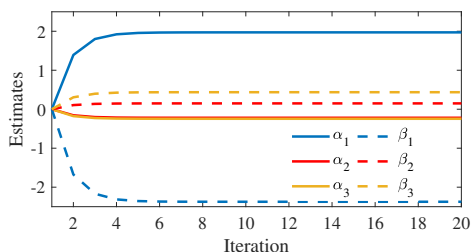


Fig. 6. Identification results: estimates versus iterations.

To identify the spatial frequency components, experiment results are recorded and analyzed. By mapping the independent variable from time to space, the frequency in spatial domain is derived, as shown in Fig. 7.

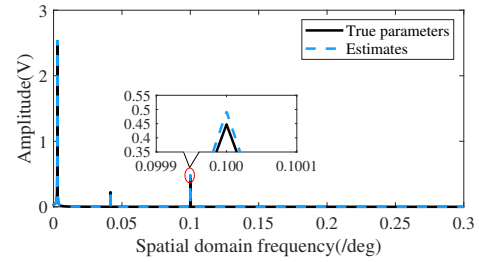


Fig. 7. Identification in spatial domain

In this case study, the parameters of the 4th-order LESO, w_{eso} and b can be calculated as

$$w_{eso} = 10\text{rad/s}, \quad b = 1000 \quad (40)$$

Table 1. Comparison results

	α_1	α_2	α_3	β_1	β_2	β_3
True parameters	1.9	-0.2	-0.2	-2.4	0.1	0.4
Estimates	1.97	-0.21	-0.24	-2.37	0.14	0.43

4.2 Comparison and simulation studies

In this example, for a better description of proposed method, a S-curve instead of a trapezoid is given in order to reduce the impulsion caused by the suddenly change of angular acceleration, shown in Fig. 8.

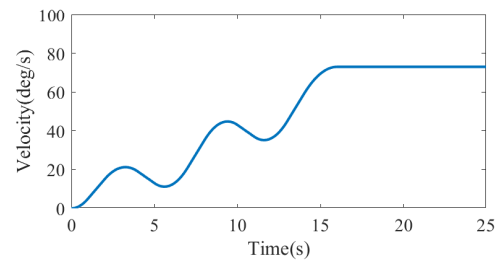


Fig. 8. Velocity reference

Simulation studies are implemented for comparison with four controllers respectively, including a basic stabilizing controller $K(s)$, a LESO, a data-driven ILC based on orthogonal projection and a compound controller combined with ILC based on orthogonal projection and LESO.

The response of the system, in which only the stabilizing controller $K(s)$ is applied, is exhibited in Fig. 9. Obviously, there exist very large ripples in the output angular position. When a 4th-order LESO is merely added, the corresponding angular position tracking error is illustrated in Fig. 10. It can be seen that the steady state error has been reduced, but its periodic disturbances remain a problem. In Fig. 11, when a data-driven ILC based on orthogonal projection algorithm is applied alone, although the periodic disturbances are reduced to a great extent, the steady error still exists. Finally, the compound controller, which is a combination of ILC and LESO, is applied and the tracking error is illustrated in Fig. 12. In the steady-state, significantly better tracking is obtained since the ripples, including the fundamental and harmonic components, are greatly suppressed, which shows a remarkable improvement over methods mentioned above.

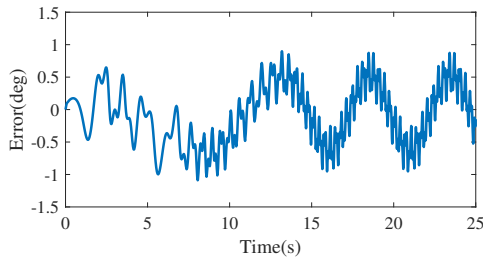


Fig. 9. Tracking error under K(s)

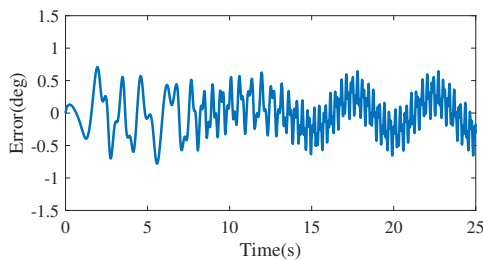


Fig. 10. Tracking error under LESO

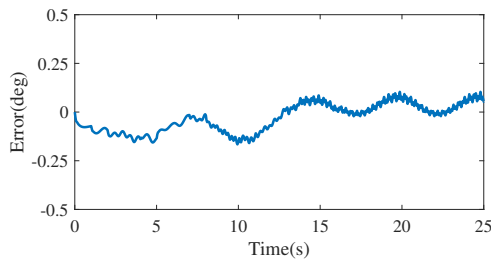


Fig. 11. Tracking error under ILC

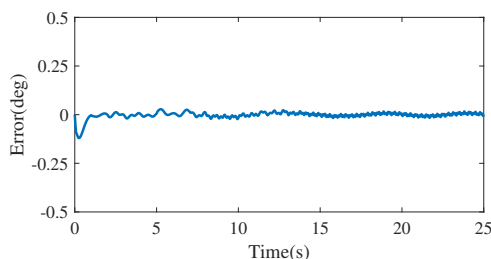


Fig. 12. Tracking error under ILC combined with LESO

The comparison results indicate that the tracking error in dynamic process is successfully attenuated by the proposed compound method.

5. CONCLUSION

This paper presents a compound control method which aims at attenuating all kinds of spatial disturbances and uncertainties. Due to the data-driven ILC, the identification matrix is greatly compressed and the complexity of the algorithm is reduced meanwhile. Besides, LESO helps a lot to enhance the performance of uncertainties suppression. The simulation results demonstrate that the proposed method effectively improves the accuracy of the ripple identification, and significantly minimizes the disturbances. Our future work is to apply the compound method to experimental research which is carried out on the actual turntable system.

REFERENCES

- Ahm, H.S., Chen, Y.Q., and Moore, K.L. (2007). Iterative learning control: brief survey and categorization. *IEEE Transactions on Systems, Man and Cybernetics, Part C*, 37(6), 1099–1121.
- Dan, W. and Chen, K. (2009). Design and analysis of precision active disturbance rejection control for noncircular turning process. *IEEE Transactions on Industrial Electronics*, 56(7), 2746–2753.
- Guemes, J.A., Iraolagoitia, A.A., and Hoyo, J.J.D. (2011). Torque analysis in permanent-magnet synchronous motors: A comparative study. *IEEE Transactions on Energy Conversion*, 26(1), 55–63.
- Han, J.Q. (2009). From pid to active disturbance rejection control. *IEEE Transactions on Industrial Electronics*, 56(3), 900–906.
- Huang, Y. and Xue, W.C. (2014). Active disturbance rejection control: Methodology and theoretical analysis. *Isa Transactions*, 53(4), 963–976.
- Huo, X., Tong, X.G., Liu, K.Z., and Ma, K.M. (2016). A compound control method for the rejection of spatially periodic and uncertain disturbances of rotary machines and its implementation under uniform time sampling. *Control Engineering Practice*, 53, 68–78.
- Huo, X., Wang, M.Y., Liu, K.Z., and Tong, X.G. (2020). Attenuation of position-dependent periodic disturbance for rotary machines by improved spatial repetitive control with frequency alignment. *IEEE/ASME Transactions on Mechatronics*, 25(1), 339–348.
- Kalyanam, K. and Tsao, T.C. (2012). Two-period repetitive and adaptive control for repeatable and nonrepeatable runout compensation in disk drive track following. *IEEE/ASME Transactions on Mechatronics*, 17(4), 756–766.
- Liu, J., Li, H.W., and Deng, Y.T. (2018). Torque ripple minimization of pmsm based on robust ilc via adaptive sliding mode control. *IEEE Transactions on Power Electronics*, 33(4), 3655–3671.
- Mishra, S. and Tomizuka, M. (2009). Projection-based iterative learning control for wafer scanner systems. *IEEE/ASME Transactions on Mechatronics*, 14(3), 388–393.
- Ou, J., Liu, Y., Qu, R., and Doppelbauer, M. (2018). Experimental and theoretical research on cogging torque of pm synchronous motors considering manufacturing tolerances. *IEEE Transactions on Industrial Electronics*, 65(5), 3772–3783.
- Stearns, H., Mishra, S., and Tomizuka, M. (2008). Iterative tuning of feedforward controller with force ripple compensation for wafer stage. In *Proceedings of the 10th IEEE International Workshop on Advanced Motion Control*, 234–239.
- Tousain, R., Eduard, V.D.M., and Bosgra, O. (2001). Design strategy for iterative learning control based on optimal control. In *Proceedings of the 40th IEEE Conference on Decision and Control*, 4463–4468.
- Xu, J.X. and Tan, Y. (2003). Linear and nonlinear iterative learning control. *Lecture Notes in Control and Information Sciences*, 291.
- Yao, W.S., Tsai, M.C., and Yamamoto, Y. (2013). Implementation of repetitive controller for rejection of position-based periodic disturbances. *Control Engineering Practice*, 21(9), 1226–1237.